Fundamentals of Next Generation Compact MOSFET Models

C. Galup-Montoro
Márcio C. Schneider
Universidade Federal de Santa Catarina
Campus Trindade – CTC–EEL–LCI
Florianopolis–SC– Brazil
+55–48–331–7720
Viriato C. Pahim
carlos@eel.ufsc.br
marcio@eel.ufsc.br
viriato@grad.ufsc.br

ABSTRACT
It has recently become clear that the electronics industry is turning away from source-referenced, threshold voltage based MOSFET models. The two main approaches as candidates to replace BSIM-type models are inversion-charge and surface-potential models.
This paper provides an overview of the basic physics that must be modeled to build a compact model for the MOSFET and compares the two approaches taken by the developers of next generation models.

Categories and Subject Descriptors
B.7.2 [**Integrated Circuits**]: Design Aids – *simulation*.

General Terms
Design, Performance.

Keywords
MOSFET model, surface potential model, inversion-charge model, compact model.

1. INTRODUCTION
The modeling of MOS transistors for integrated circuit design has been driven by the needs of digital circuit simulation for many years. The present trend toward mixed analog-digital chips creates a necessity for MOSFET models appropriate for analog and RF design as well [1, 2, 3, 4]. For example, using a source-referenced threshold voltage makes it hard to properly model the intermodulation in passive mixers [4].
Strong inversion used to be the prevailing MOS operation region, but as a consequence of the technological trend toward shorter channel lengths, off-state leakage constraints, and reduced supply voltages, MOS devices now often operate in the moderate and weak inversion regions [5]. A representative example of a circuit that employs MOSFET´s operating in either weak inversion or moderate inversion is the self-biased current source described in [18].

SBCCI'05, September 4–7, 2005, Florianópolis, Brazil.

Conventional models, such as BSIM [6], are direct models since the drain current and the terminal charges are explicit functions of the terminal voltages. Since these direct models use mathematical smoothing functions to describe the transition between weak and strong inversion, they are not accurate enough to represent the moderate inversion region, widely employed in low supply voltage circuits [3, 4].
Currently, there are essentially two alternative approaches to direct models, namely surface-potential-based (ϕ_s-based) [1, 3, 4] and inversion-charge-based (Q'_I-based) [2, 7, 8, 9, 10] models. In these two indirect models, the drain current and the terminal charges are indirect functions of the terminal voltages through either the surface potential or the inversion charge density.
Conventional surface potential models based on the original charge-sheet approximation of Brews [14] do not lead to a practical result due to difficulties in introducing velocity saturation effects for short-channels and obtaining closed-form self-consistent charges for the device terminals. Practical compact ϕ_s-based models (MM11, SP) use linearization of the surface potential vs. inversion charge density in a similar way as Q'_I-based models do [3, 4].
With regard to Q'_I-based models, the inversion charge density is approximated using the unified charge control model (UCCM) [8].
Briefly, ϕ_s-based and Q'_I-based models have a common background, but enough differences between them exist to motivate model developers to support either approach. Because the complete transistor model, including the different physical effects relevant to advanced technologies, is very complex, we will reduce our comparison to the core models based on either surface potential or inversion charge.

2. PAO AND SAH EXACT I-V MODEL
For a long-channel device, the *gradual channel approximation* [3, 11] is valid, i.e., the longitudinal (x-direction) component of the electrical field can be assumed to be much smaller than the transversal (y-direction) component.
For the calculation of the current I_{DS} that flows from drain to source, it is assumed that the hole current (for an n-channel) as well as recombination/generation can be neglected [3,11]. In the ideal case, it is furthermore assumed that there is a current flow in the x-direction only. Assuming the mobility μ to be independent of bias and position, the channel current can be written [11, 12] as

$$I_{DS} = -\mu W Q_I' \frac{dV_C}{dx} \qquad (1)$$

where W is the transistor width, V_C is the channel–to-substrate potential and Q'_I is the inversion charge density.
Integrating (1) along the channel, from source to drain, [11, 12] yields:

$$I_{DS} = -\frac{\mu W}{L}\int_{V_S}^{V_D} Q'_I dV_C \tag{2}$$

where L is the channel length. Expression (2) is very general and includes both the drift and diffusion mechanisms, thus giving an exact model of the classical (as opposed to quantum mechanical) long channel MOSFET.
Because there is no general analytically integrable expression for the inversion charge density in terms of the channel potential, the conventional approach has been to develop separate models for strong and weak inversion, where simple expressions, linear and exponential, respectively, for the inversion charge density are available. The complete model is then obtained with the aid of interpolation functions to describe the transition between weak and strong inversion. This approach, that was widely used to obtain models for electrical simulation, including BSIM4, is no longer considered appropriate for advanced MOS technologies.
To obtain a general analytical expression for the current, (2) can be calculated by means of a change of variable. Two alternatives are currently available, namely surface potential models, based on (3), and inversion charge models, based on (4)

$$I_{DS} = -\mu\frac{W}{L}\int_{\phi_{s0}}^{\phi_{sL}} Q'_I(\phi_s)\frac{dV_C}{d\phi_s}d\phi_s \tag{3}$$

$$I_{DS} = -\mu\frac{W}{L}\int_{Q'_{IS}}^{Q'_{ID}} Q'_I\frac{dV_C}{dQ'_I}dQ'_I \tag{4}$$

A similar procedure can be applied to calculate the total charges.

3. SURFACE POTENTIAL MODEL

To calculate (3), $Q'_I(\phi_S)$ can be determined from the *charge-sheet approximation.* In this approximation, the potential drop across the inversion layer is ignored for the calculation of the bulk charge density Q'_B. Consequently, the inversion charge density, for an n-channel, Q'_I is expressed as [11, 13]:

$$Q'_I = -C'_{ox}\left(V_G - V_{FB} - \phi_s - \gamma\sqrt{\phi_s - \phi_t}\right) \tag{5}$$

where C'_{ox} is the oxide capacitance per unit area, γ is the body factor and V_G, V_{FB} and ϕ_t are the gate, flatband and thermal voltages, respectively.
$dV_C/d\phi_S$ is determined from the implicit relation for the surface potential [3, 11]:

$$\left(V_G - V_{FB} - \phi_s\right)^2 = \gamma^2\left(\phi_t e^{(\phi_S - 2\phi_F - V_C)/\phi_t} + \phi_s - \phi_t\right) \tag{6}$$

where ϕ_F is the Fermi potential of the bulk. (6) is very accurate for $\phi_S > 6\phi_t$. Near flatband (6) must be modified to includ the term for the hole density.

Differentiating (6) with respect to ϕ_s we obtain [13, 15]

$$\frac{dV_C}{d\phi_s} = 1 + \phi_t\frac{2\left(V_G - V_{FB} - \phi_s\right) + \gamma^2}{\left(V_G - V_{FB} - \phi_s\right)^2 - \gamma^2\left(\phi_s - \phi_t\right)} \tag{7}$$

Substituting (5) and (7) into (3) we arrive at

$$I_{DS} = \mu\frac{W}{L}C'_{ox}\int_{\phi_{s0}}^{\phi_{sL}}\left[V_G - V_{FB} - \phi_s - \gamma\sqrt{\phi_s - \phi_t}\right]d\phi_s + \\ + \mu\frac{W}{L}C'_{ox}\int_{\phi_{s0}}^{\phi_{sL}}\left[\phi_t\frac{2\left(V_G - V_{FB} - \phi_s\right) + \gamma^2}{V_G - V_{FB} - \phi_s + \gamma\sqrt{\phi_s - \phi_t}}\right]d\phi_s \tag{8}$$

(8) allows deriving an explicit general equation for the current [13], but the final expression is rather cumbersome. The result can be simplified by noting that the last term in the right-hand side of (8) is relevant for small Q'_I only (weak inversion) [15]. The application of this approximation to (8) results [15] in:

$$I_{DS} = \mu\frac{W}{L}C'_{ox}\int_{\phi_{s0}}^{\phi_{sL}}\left[V_G - V_{FB} - \phi_s - \gamma\sqrt{\phi_s - \phi_t}\right]d\phi_s + \\ + \mu\frac{W}{L}C'_{ox}\int_{\phi_{s0}}^{\phi_{sL}}\left[\phi_t\left(1 + \frac{\gamma}{2\sqrt{\phi_s - \phi_t}}\right)\right]d\phi_s \tag{9}$$

Integration of (9) is straightforward, the result being known as Brews' charge-sheet model [14].
Most advanced surface potential models [3, 4] introduce an additional approximation, substituting the depletion charge density term with the first two term of the Taylor expansion around a certain value of the surface potential ϕ_{se}. The charge sheet current expression is then written in terms of the surface potential values at the boundaries of the channel as follows [11]:

$$I_{ds} = I_{drift} + I_{diff} \tag{10a}$$

$$I_{drift} = -\frac{W}{L}\cdot\mu\cdot\left(\overline{Q'_i} - \alpha\cdot C'_{ox}\cdot\left(\phi_{se} - \frac{\phi_{SL} + \phi_{S0}}{2}\right)\right)\cdot \\ \cdot\left(\phi_{SL} - \phi_{S0}\right) \tag{10b}$$

$$I_{diff} = \frac{W}{L}\mu C'_{ox}\alpha\phi_t\left(\phi_{SL} - \phi_{S0}\right) \tag{10c}$$

where

$$\alpha = 1 + \frac{\gamma}{2\cdot\sqrt{\phi_{se} - \phi_t}} \tag{11}$$

$$\overline{Q'_i} = -C'_{ox}\cdot\left(V_{GB} - V_{FB} - \gamma\cdot\sqrt{\phi_{se} - \phi_t} - \phi_{se}\right) \tag{12}$$

Choosing $\phi_{se} = \frac{1}{2}(\phi_{SL} + \phi_{S0})$ [3, 4] the surface potential-based expression (10) is simplified. Another virtue of this choice of ϕ_{se} is that the resulting model is inherently symmetric [3,4].

4. INVERSION CHARGE BASED MODELS

In the inversion charge based model (4), the term dVc/dQ'_I is calculated from the unified charge control model (UCCM) [8]. The UCCM model can be readily derived from the description of the three-terminal MOS structure through a capacitive model as shown in Fig. 1.

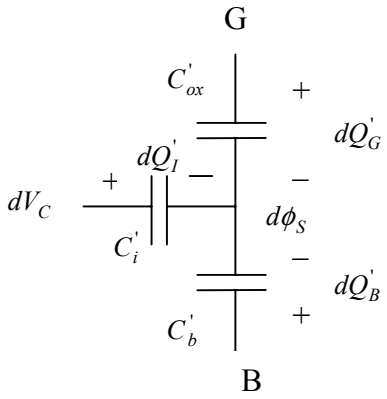

Figure 1: Small-signal model for the three-terminal MOSFET

UCCM follows from the two following approximations:

1. the depletion capacitance per unit area C'_b is assumed to be constant along the channel and is calculated assuming the inversion charge to be negligible in the potential balance equation;
2. the inversion capacitance is proportional to the inversion charge density ($C'_i = -Q'_I/\phi_t$). This hypothesis is equivalent to that used to obtain (9) from (8).

It follows that [16]

$$dQ'_I\left(\frac{1}{nC'_{ox}} - \frac{\phi_t}{Q'_I}\right) = dV_C \qquad (13)$$

where $nC'_{ox} = C'_{ox} + C'_b$

Equation (13) represents the UCCM in differential form. Substituting (13) into (4) yields

$$I_{DS} = -\mu\frac{W}{L}\int_{Q'_{IS}}^{Q'_{ID}} Q'_I\left(\frac{1}{nC'_{ox}} - \frac{\phi_t}{Q'_I}\right)dQ'_I \qquad (14)$$

Integrating (14) from source to drain results in

$$I_{DS} = \frac{\mu W}{L}\left[\frac{Q'^{\,2}_{IS} - Q'^{\,2}_{ID}}{2nC'_{ox}} - \phi_t\left(Q'_{IS} - Q'_{ID}\right)\right] \qquad (15)$$

In (15) the quadratic term corresponds to the drift currents and the linear term to the diffusion current. The slope factor n in (15) is given by $n = 1 + \gamma/2\sqrt{\phi_{sa} - \phi_t}$, with ϕ_{sa} being equal to the surface potential calculated from (5) assuming the inversion charge to be negligible.

5. COMPARISON BETWEEN MODELS

The numerical calculation of the Pao-Sah double integral (2) will be used as a baseline for the comparison of the current models. The inversion charge in (2) is solved by finite differences with a non-uniform discrete mesh in y.

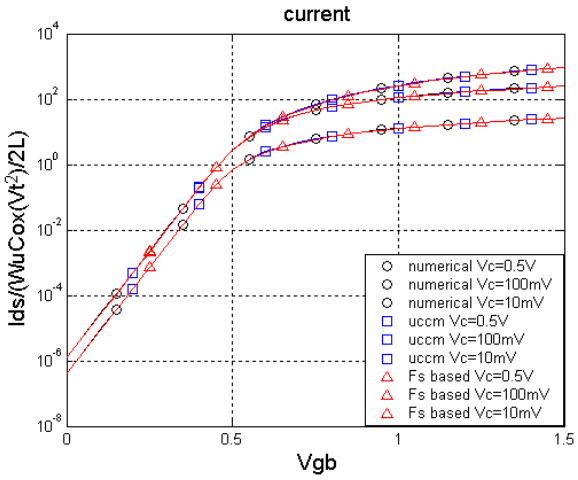

Figure 2: Normalized drain current

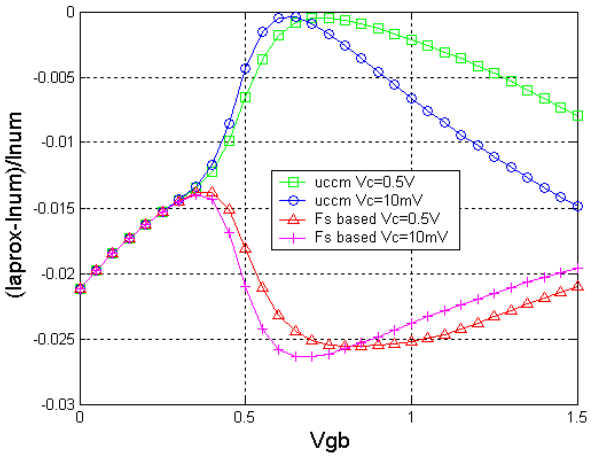

Figure 3: Error in the drain current. The Pao-Sah model is used as reference.

For the simulations, the following parameters were used: temperature = 27 °C, oxide thickness = 2nm, doping concentration = 2E18 cm^{-3}.

As shown in Figs. 2-3, the inversion charge and the ϕ_s-based models give very good approximations for the drain current from weak, through moderate to strong inversion. Also, note that the

Q'_I - and the ϕ_s-based models are strictly equivalent in weak inversion. (the equivalence between the models in weak inversion will be explained in annex B). An interesting result from Fig. 3 is that the charge model gives a better approximation than the charge-sheet model for moderate inversion while in strong inversion the errors are roughly the same.

6. CONCLUSIONS

Two approaches to MOSFET compact models have been described. The future direction for the industry is still unclear. The Compact Model Council is currently examining examples of both types and their work will provide additional insight into the consequences of various modeling choices. Ultimately, engineers responsible for providing models to meet the needs of circuit designers will decide which model to use.

7. ACKNOWLEDGEMENT

The authors are particularly indebted to Dr. Rafael Rios for his part in this work. His suggestions during its progress, his help with the numerical simulations and his assistance with the manuscript have contributed materially to the appearance of this paper.

8. ANNEX A: CALCULATION OF THE SURFACE POTENTIAL

The gate electrode charge per unit area is given by [11]:

$$Q'_G = C'_{ox}\left(V_G - V_{FB} - \phi_s\right) \tag{A1}$$

The general implicit relation for the surface potential is [3, 11]:

$$\left(V_G - V_{FB} - \phi_s\right)^2 = \gamma^2\phi_t e^{-(2\phi_F+V_C)/\phi_t}\left(e^{\phi_s/\phi_t} - 1\right) + \\ + \gamma^2\left(\phi_s + \phi_t\left(e^{-\phi_s/\phi_t} - 1\right)\right) \tag{A2}$$

The *charge-sheet approximation* neglects the potential drop across the inversion layer for the calculation of the bulk charge density Q'_B. According to the charge-sheet approximation, Q'_B is given by

$$Q'_B = -sign(\phi_s)C'_{ox}\gamma\sqrt{\phi_s + \phi_t\left(e^{-\phi_s/\phi_t} - 1\right)} \tag{A3}$$

Expression (A3) gives a continuous model from accumulation through depletion to inversion. The inversion charge density Q'_I is expressed as

$$Q'_I = -C'_{ox}\left(V_G - V_{FB} - \phi_s + \frac{Q'_B}{C'_{ox}}\right) \tag{A4}$$

For ϕ_s-based models, one can calculate ϕ_s iteratively using (A2) [17] and the resultant value is used to calculate Q'_G, Q'_B and Q'_I from (A1), (A3) and (A4), respectively.

9. ANNEX B THE UNIFIED CHARGE CONTROL MODEL

The channel charge density for which the diffusion current equals the drift current is designated the **pinch-off charge density** Q'_{IP}.

$$Q'_{IP} = -nC'_{ox}\phi_t \tag{B1}$$

The channel-to-substrate voltage (V_C) for which the channel charge density equals Q'_{IP} is called the **pinch-off voltage** V_P.
The pinch-off voltage is given [2] by:

$$V_P = \phi_{Sa} - 2\phi_F - \phi_t\left(1 + \ln\left(\frac{n}{n-1}\right)\right) \tag{B2}$$

UCCM is given by [2]

$$V_P - V_C = \phi_t\left[\frac{Q'_{IP} - Q'_I}{nC'_{ox}\phi_t} + \ln\left(\frac{Q'_I}{Q'_{IP}}\right)\right] \tag{B3}$$

A fundamental property of (B3) is that, in weak inversion, it is asymptotically coincident with the surface potential charge-sheet model. Substituting (B1) and (B2) into (B3) and considering $Q'_I \to 0$, it follows that

$$Q'_I = -\frac{\sqrt{2q\varepsilon_S N_A}}{2\sqrt{\phi_{sa} - \phi_t}}\phi_t e^{(\phi_{sa}-2\phi_F)/\phi_t} e^{-V_C/\phi_t} \tag{B4}$$

In Fig. 4, we illustrate the results of the inversion charge density obtained numerically, using the charge-sheet model, or UCCM$^+$, an improved version of the UCCM, which includes the additional term ϕ_t into the bulk charge. UCCM$^+$ and the ϕ_s-based model give very good approximations for the inversion charge densities from weak, through moderate to strong inversion. For the simulations in Fig. 4, Fig. 5, and Fig. 6, the following parameters were used (unless specified otherwise): temperature = 27 ^{o}C, oxide thickness = 2nm, doping concentration = 2E18 cm^{-3}.

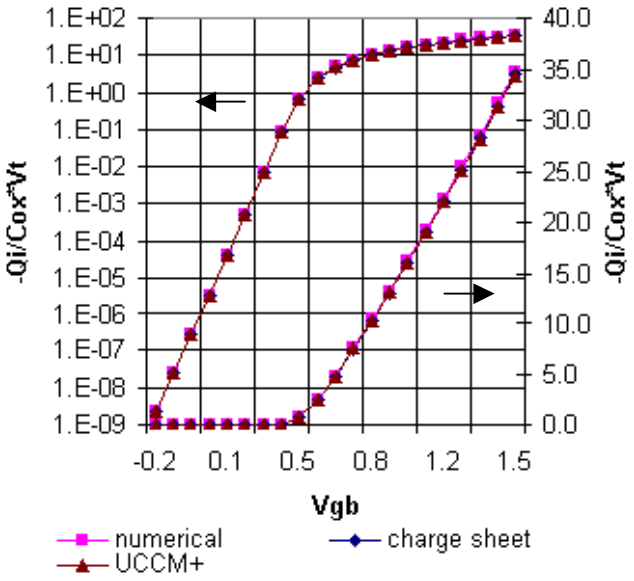

Figure 4: Inversion charge density

As shown in Fig. 5 and Fig.6, both ϕ_s-based charge-sheet model and UCCM$^+$ approaches give errors less than 3% under normal bias conditions and for a wide range of physical parameters. UCCM$^+$ and charge sheet are strictly equivalent in weak inversion as expected. An interesting result from Figs. 5 and 6 is that UCCM$^+$ gives a better approximation than the charge-sheet model for moderate inversion while in strong inversion the opposite is observed. The better accuracy of the UCCM$^+$ in moderate inversion is related to the fact that the capacitive model on which the UCCM$^+$ is based is more general than the charge-sheet approximation. In strong inversion the value of the inversion capacitance ($-Q_I' / \phi_t$) used in UCCM$^+$ is less accurate and the charge-sheet model gives a better result.

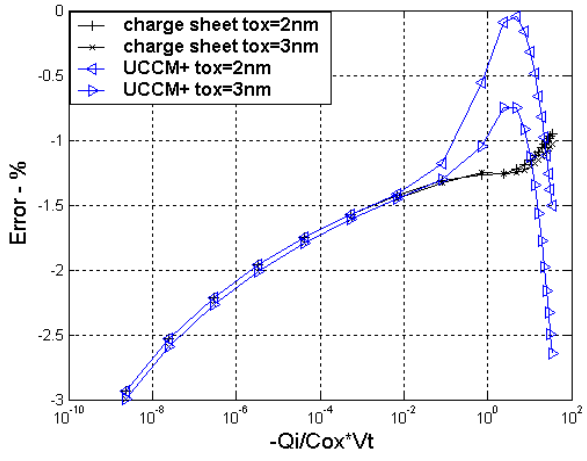

Figure 5: Error in inversion charge density for two doping concentrations

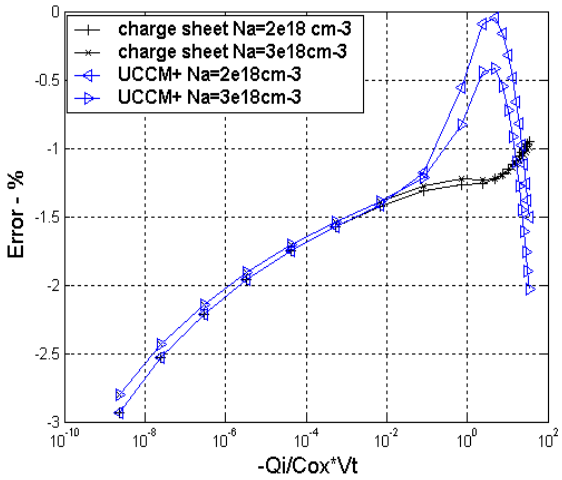

Figure 6: Error in inversion charge density for two oxide thicknesses

10. REFERENCES

[1] M. Miura-Mattausch, U. Feldmann, A. Rahm, M. Bollu, and D. Savignac, "Unified complete MOSFET model for analysis of digital and analog circuits," *IEEE Trans. Computer-Aided Design*, vol. 15, pp. 1–7, January 1996.

[2] C. Galup-Montoro, M. C. Schneider, and A. I. A. Cunha, "A current-based MOSFET model for integrated circuit design," Chapter 2 of Low-Voltage/Low-Power Integrated Circuits and Systems, pp 7-55, edited by E. Sánchez-Sinencio and A. Andreou, IEEE Press, 1999.

[3] R. van Langevelde, A. J. Scholten, and D. B. M. Klaassen, "Physical background of MOS model 11**",** Nat. Lab. Unclassified Report 2003/00239. April 2003. (available on line at http://www.semiconductors.philips.com/Philips_Models/)

[4] G. Gildenblat, H. Wang, T.-L. Chen, X. Gu, and X. Cai, "SP: An advanced surface-potential-based compact MOSFET model", *IEEE J. Solid-State Circuits*, vol. 39, no. 9, pp. 1394-1406, September 2004.

[5] C. Enz, F. Krummenacher and E. A. Vittoz, "An analytical MOS transistor model valid in all regions of operation and dedicated to low-voltage and low-current applications," *Analog Integrated Circuits and Signal Processing Journal*, vol. 8, pp. 83-114, July 1995.

[6] W. Liu *et al.*. (1999) BSIM3v3 Manual. Dept. Elect. Eng. Comp. Sci., Univ. California, Berkeley. [Online]. Available: http://wwwdevice.eecs.berkeley.edu/~bsim3/get.html

[7] M. A. Maher and C. A. Mead, "A physical charge-controlled model for MOS transistors," in *Advanced Research in VLSI*, P. Losleben (ed.), MIT Press, Cambridge, MA, 1987.

[8] Y. Byun, K. Lee and M. Shur, "Unified charge control model and subthreshold current in heterostructure field effect transistors," *IEEE Electron Device Letters*, vol. 11, no. 1, pp. 50-53, January 1990.

[9] J.-M. Sallese, M. Bucher, F. Krummenacher, and P. Fazan, "Inversion charge linearization in MOSFET modeling and

rigorous derivation of the EKV compact model", *Solid-State Electronics* vol. 47, pp. 677–683, 2003.

[10] J. He, X. Xi, M. Chan, A. Niknejad, and C. Hu, "An advanced surface potential-plus MOSFET model," p. 262 in *Tech. Proc. 2003 Nanotechnology Conf.*

[11] Y. Tsividis, *Operation and modeling of the MOS transistor*, 2nd edition, McGraw-Hill, New York, 1999.

[12] H. C. Pao and C. T. Sah, "Effects of diffusion current on characteristics of metal-oxide (insulator)-semiconductor transistors," *Solid-State Electronics*, vol. 9, pp. 927-937, 1966.

[13] G. Baccarani, M. Rudan and G. Spadini, "Analytical i.g.f.e.t. model including drift and diffusion currents", *Solid-state and Electron Devices*, vol. 2, no. 2, pp. 62-68, March 1978.

[14] J. R Brews, "A charge sheet model for the MOSFET," *Solid-State Electronics*, vol.21, pp.345-355, 1978.

[15] F. Van de Wiele, "A long-channel MOSFET model", *Solid-State Electronics*, vol. 22, no. 12, pp. 991-997, December 1979.

[16] A. I. A. Cunha, M. C. Schneider, and C. Galup-Montoro, "Derivation of the unified charge control model and parameter extraction procedure," *Solid-State Electronics*, vol. 43, no 3, pp. 481-485, March 1999.

[17] R. Rios, S. Mudanai, W.-K. Shih, and P. Packan, "An efficient surface potential solution algorithm for compact MOSFET models," pp 755-758. *IEDM 2004 Tech. Dig*.

[18] E. M. Camacho-Galeano, C. Galup-Montoro and M. C. Schneider, "A 2-nW 1.1-V self-biased current reference in CMOS technology", *IEEE Transactions on Circuits and Systems II: Express Briefs*, vol. 52, no. 2, pp. 61-65, February 2005.